Measurement of the Quenching Factor for Barium Fluoride Crystals

Ariel Hasse
Professor David Hitlin
California Institute of Technology

1 Abstract

The energy of particles can be determined by measuring the scintillation light emitted by crystals such as barium fluoride. As the particles travel through the inorganic scintillator, Birks Law describes the amount of light emitted for a given energy lost. The ratio of dispersed energy is dependent on the mass of the particle; this is known as the quenching factor. Barium fluoride has two mechanisms of scintillation, a fast and a slow component, which are at different wavelengths, that determine how quickly photons are emitted. The ratios of energy from the fast and slow components from multiple photomultiplier tubes with varying quantum efficiency as a function of wavelength, determine the final quenching factor. We find that the quenching factors of the fast and slow components are substantially different. We measure the response of the barium fluoride crystal fast and slow components to alpha particles of known energies coming from the decay of slight radium contamination in the crystals. Confirmation with the known values allows for analysis of energy readout from gamma, electron, and alpha particles. This data, along with the quenching factor, is valuable for many high-energy physics experiments in which inorganic scintillators are used to find the mass or energy of particles. We will also use the findings to study the physical mechanisms affecting the quenching factor.

2 Introduction

Scintillation is light emitted by a material absorbing a particles energy. These materials, known as scintillators, can be both organic or inorganic. Electrons in crystals, which are inorganic, are excited from the valance band by the deposited energy of a particle to either the conductance band or the exciton band. When electrons leave the valence band they leave a gap in the energy level. This gap, known as an electron hole, forms a pair with the electron and the pair traverses through the scintillator until an impurity in the crystal captures the instability.The impurities in scintillators have electronic levels in between the valence and exciton bands in the crystals. Once the electron-hole pair is captured the impurity deexcites by emitting scintillation. When the electron in the electron-hole pair is captured from the exciton band its known as the fast component and conductive band its known as the slow component. The fast component emits light more quickly, since the conductive band electrons reach a phenomenon known as a metastable state where the atomic system does not immediately decay to the state of least energy, thereby not immediately emitting a photon.

Using photodectors scintillation can be detected. The amount of scintillation is linearly proportional to the energy deposited and the slope of the line correlates to particles' mass and energy. This relationship is used in particle physics expeirments, like those at Fermi Lab, to detect and diffrentiate new particles. This system is referred to as the calorimeter and is made of crystals with adjacent photodectors.

Barium Flouride (BaF_2) crystals, a type of inorganic scintillator, are of particular interest because of its exceptional fast component. For BaF_2 crystals the fast component is .6 ns and the slow component is 540 ns. BaF_2's fast component emits light more quickly than any other scintillator of its kind. A short decay mechanism provides more precision, proportional to the $\sqrt{\tau}$ where τ is the scintillation time, and allows for more successive events to be detected. In order to benefit from the short decay time the scintillation light from the fast component must be seperated from the slow component. The relationship can be described by the non-linear energy loss through the lattice, known as Birk's constant or the quenching factor (α_Q).

Birk's Law describes how energy is lost as a function of light loss

$dL/dx = S * (dE/dx)/(1 + \alpha_Q * (dE/dx))$

where L is the amount of light detected, E is the energy of the particle, and S is a constant specific to the crystal. The quenching factor is linearly dependent on energy and is different for the fast and slow component. We assume the relationship is in the form of

$\alpha_Q = E_f * \alpha_f + E_s * \alpha_s$

where α_Q is the quenching factor for a given light detector and energy level, E_f and E_s are the proportions of fast and slow scintillation, respectively, where $E_f + E_s = 1$, and α_f and α_s are the quenching factors for the fast and slow component at a given energy. Birk's constant is affected by non-linearly by the mass and linearly by the energy of a particle. Despite scintillators' supposed linear proportion between energy deposited and light emitted, as particles increase in mass the quenching factor increases. $E_f + E_s = 1$ is determined from the convolution of the Barium Flouride Emission spectrum and the quantum efficiency (QE)of the photodector.

The quenching factors for the fast ans slow components as a function of energy are determined using at least two photodectors. The expected linearity, calibration factor, can be determined using low mass decays such as gamma or electron sources with known keV values. The calirbation is the slope of known energy versus the measured energy from the sensor. Birk's constant, as a function of deposited energy, is determined from the measured scintillation of heavier particles, which are affected by non-linear energy loss, as a quotient of the known energy and the expected energy after the calibration factor is applied.

$\alpha_Q = (KnownEnergyinkeV)/(RecordedEnergy * CalibrationFactor)$

This is repeated for each sensor at each energy level and

$\alpha_Q = E_f * \alpha_f + E_s * \alpha_s$ is plotted α_f versus α_s

for each detector. The point of best intersection represents the quenching factor for the slow and fast component. Replacing the α_f with the total α_Q in Birk's Law then determines the scintillation from the fast component at a given energy.

In our research we determined Birk's constant for the fast and slow component

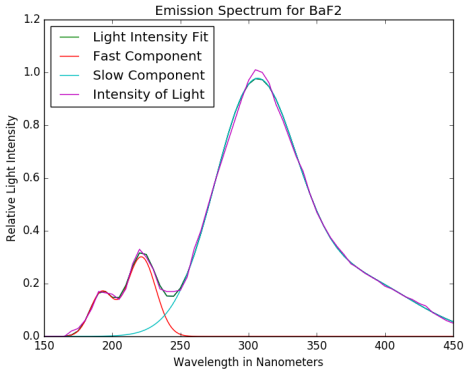

Figure 1: Fitted Emission Spectrum for BaF_2 crystals

of BaF_2 for alpha particles at energies 4.8, 5.5, 6.0, and 7.7 MeV. We found α_Q, E_f, and E_s for three photodectors, in our case Photomultiplier Tubes (PMTs). α_Q was determined with low mass particles from four radioactive sources and $E_f + E_s = 1$ was determined from integrating under the curve of the QE and BaF_2 emission specturm convolution.

The collected data and the subsequent analysis yield

$\alpha_s = -0.1398072 * Energy + 4.13497323$ and $\alpha_f = -0.45007859 * Energy + 11.23363402$

with errors of

$\sigma_s = [1.36287, 1.31089, 1.2333, 1.10977]$ and $\sigma_f = [0.0290772, 0.0310162, 0.0319127, 0.0313639]$.

These functions can be used in future high energy physic experiments to isolate the fast component in BaF_2. Beyond experimental analysis on the quenching factor, the physical phenomenom that determine the constant will be explored.

3 Method

Due to the experimental nature of our research we describe the method for the two main processes: data collection and data analysis. Experimentally we find the center of energy peaks for each PMT with each source. In the analysis process we found the calibration factors and the quenching factors using our measurements and manufacturer's data.

3.1 Laboratory Equipment and Configuration

The final experiment used three Photomultiplier Tubes; ultraviolet extended full spectrum, solarblind, and ultraviolet extended full spectrum with a shortpass filter. For both PMTs and the filter the manufacturer has provided the light intensity as a function of photon wavelength. We also used five radioactive sources. Four of the sources were low mass decays, electron or gamma; AmericiumBerillyum 241 (AmBe 241), Cesium 137 (Cs 137), Cobalt 60 (Co 60), and Sodium 22 (Na 22). Both Na 22 and Co 60 have particle decays at two energy peaks which provided six points for calibration [Figure 2]. The fifth source is

Source	Cs 137	Na 22 First Peak	Na 22 Second Peak	Co 60 First Peak	Co 60 Second Peak
Energy (keV)	662	511	1274	1170	1330
Source	**AmBe 241**	**Ra 226 First Peak**	**Ra 226 Second Peak**	**Ra 226 Third Peak**	**Ra 226 Fourth Peak**
Energy (keV)	59	4800	5500	6000	7700

Figure 2: Table for each source used and its corresponding keV value

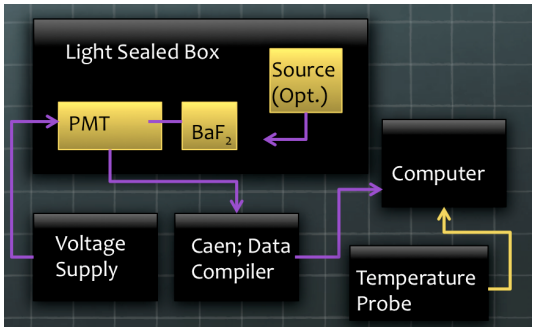

Figure 3: Equipment schematic for experiments

alpha decay from natural Radium 226 impurities in the BaF_2 crystal, which has four energy peaks. The crystal used in each experiment remained the same. It had previously been found to have a relatively high concentration of impurities which allowed for more alpha decay counts.

In addition to our variables we used several pieces of equipment to collect data. The data compiler, caen, provides a clear user interface and was designed for physics problems of this kind. The power for the PMTs was supplied by a voltage box that could be set to up to 5000 volts. We also used an arduino circuit board and two A2302 temperature probes to collect the temperature in the laboratory while tests were active. Lastly the PMT, crystal, and source was in a light sealed box with cable panels to connect equipment inside and outside [Figure 3].

3.2 Experimental Procedure

In total each source was recorded with each PMT. Before recording any sources, the PMT must be supplied the desired voltage for 12 hours. As the PMT warms up the quantum efficiency is altered and after due time, 12 hours in our case, the PMT's temperature stabilizes. The arduino probe's temperature record was also launched to ensure the PMT was not affected from external heat fluctuations.

For a given PMT the voltage and settings on the caen data compiler remain the same for each source. Depending on the quantum efficiency of the PMT we set the voltage to maximize the gain and minimize background noise; the higher the voltage, the higher the gain. The threshold, bin size, and gate length were also set. Raising the threshold

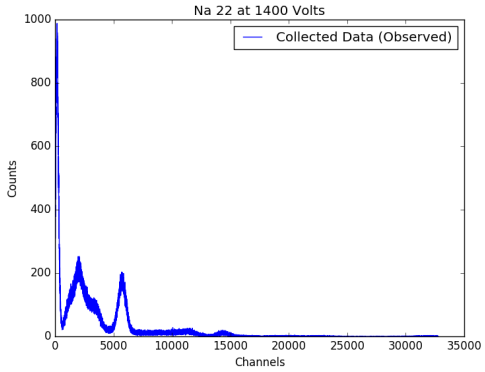

Figure 4: Na 22 Solarblind PMT total energy histogram

diminishes background noise, but can also dimish noise from the source. The bin size sets a relative scale for the energy counts and must take into account the dispersion of source peaks so the highest source is not above the recorded channel. The gate length is in ns and regulates the amount of light detected for each collection point; it can also be used to lower the portion of the slow component seen.

3.2.1 Evaluating a PMT

To begin collection with a PMT the lense and crystal are both cleaned. The crystal is then wrapped on 5 of the faces with a shielding material to prevent light from leaving out the sides and not into the PMT. The open face of the crystal is secured onto the PMT with grease to optimize light collected. Then the PMT and crystal are placed in the light sealed box and connected with coaxial cables to the voltage supply and caen. After the PMT has been left on for at least 12 hours the sources can be evaluated. Following standard radiation safety procedure we then place a source in the light sealed box within a couple inches of the crystal to increase interactions. Once the parameters are adequately set, laboratory temparature is being recorded, and data points are being collected the energy spectrum is recorded. When the caen has enough counts in each bin to show an energy peak in the histogram at the desired resolution, data is saved, and we repeat the process with the three other sources and then the crystal alone with the PMT for Ra 226.

Each source varies in rate of decay and each PMT varies in the amount of light it can record. Tests varied widely in length required to record enough data points for the histogram. In order to complete a trial the energy peaks had to be visible above the background noise and have a reasonable resolution. The initital histogram shows the number of counts at each energy level. In the data analysis each energy peak will be isolated and the position recorded as the channel value for that specific set-up [Figure 4].

3.3 Data Analysis

Before begining data collection we created unique python scripts to analyze our anticpated data. The first program extracts the histogram for each source from a txt file and fits the energy peaks with a Gaussian. The gaussian fit produces the central peak value in channels for each energy level. Then the known decay values for each source are used to find the conversion from channels to keV. The conversion is the slope of the line of best fit between each point. The conversion for each Ra 226 peak produces the expected keV value from channels in the following manner:
$ExpectedEnergyinkeV = (RecordedEnergy * 1/(conversion))$.

This is then compared to the known Ra 226 decays in keV to find the quenching factor, α_Q at each energy. We repeated this process for each PMT and recorded the quenching factors.
$\alpha_Q = (KnownEnergyinkeV)/(RecordedEnergy * CalibrationFactor)$

The second program is also repeated for each PMT. The script convolves the QE specifications from each PMT manufacturer and the emission spectrum for Barium Fluoride which produces a four gaussian representation of the fast and slow component proportions. The proportion of area from each component produces E_s and E_f.

Lastly a final script requires the input of the quenching factor and component proportions as global lists. The subsequent functions then produce four energy plots of $\alpha_Q = E_f * \alpha_f + E_s * \alpha_s$ where α_Q uses data from each PMT. The closest intersection of the line represents (α_s, α_f), the final quenching factors. To find these points we created a mathematica script and solved the minimized cost function analytically. From this process the covariance matrix can be formed to determine the errors on each value. The four (α_s, α_f) and their respective (σ_s, σ_f) are then imported back to the python script to plot each fast and slow value against the corresponding energies for the final quenching factors as a function of energy in MeV.

4 Results

We found α_Q, E_f, and E_s for each PMT. α_f and α_s were determined at the four Ra 226 energy peak values, 4.8, 5.5, 6.0, and 7.7 MeV. The fast and slow proportion was also found for each PMT. For each PMT we fit every source with a Gaussian Fits [Figures 5 and 6] which yielding the following parameter fits [Figure 7].

Energy (keV)	60	511	662	1170	1274	1330
Filter (peak channel)	Not Recorded	3200	4510.3	7908	7991	8243.4
UV (peak channel)	304	2343.6	3445	5772.8	6373.4	6648.8
Solarblind (peak channel	694.6	6183	8827	Not Recorded	13728.3	Not Recorded
Filter (sigma channel)	Not Recorded	226	245.9	349	372.8	398.8
UV (sigma channel)	59.6	138	163.7	560.1	224.8	239.8
Solarblind (sigma channel)	3 Not Recorded 40.5	794	1049.4	Not Recorded	2116.1	Not Recorded

Figure 7: Table with the recorded gaussian fit parameters

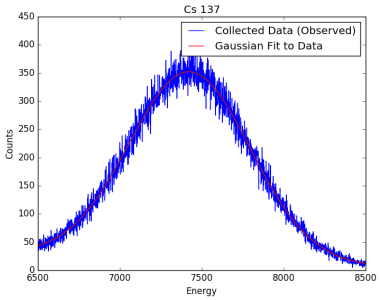

Figure 5: An Example of a Gaussian Fit, UV PMT

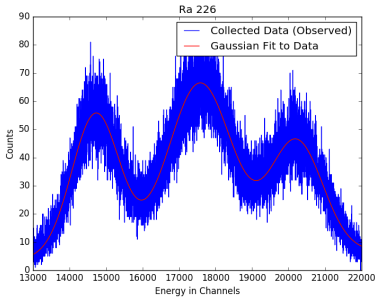

Figure 6: An Example of a Gaussian Fit, UV PMT

Using the peak value and sigma the keV to channels conversion [Figures 8 to 10] was determined for each PMT; UV with shortpass filter, UV, Solarblind = [6.33012509, 4.984, 12.0694256]

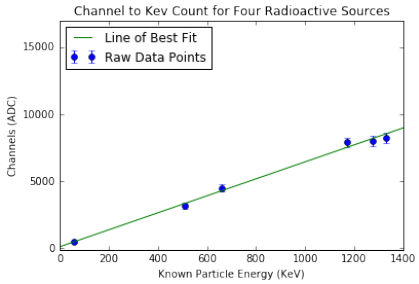

Figure 8: UV with filter Calibration Function

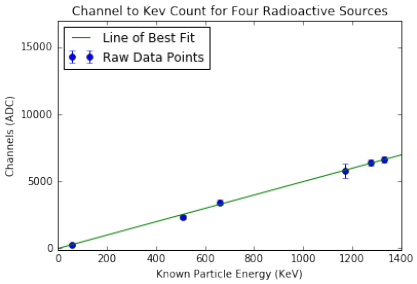

Figure 9: UV Calibration Function

The inverse slope of the best fit line multiplied by the Ra 226 peak channel values yielded the expected keV values, which then determined the quenching factors α_Q [Figures 11 to 13].

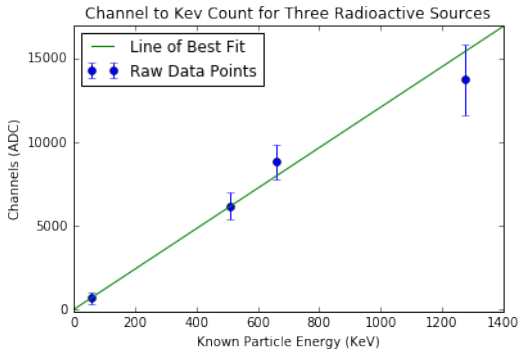

Figure 10: Solarblind Calibration Function

Quenching Factor UV with filter = [2.9762807168446512, 2.8493222446691253, 2.7046015279015254, 2.459904200468519] Quenching Factor UV = [3.269623267619078, 3.1364744649952887, 2.9771822748456365, 2.702319438114875] Quenching Factor Solarblind = [5.155991131280197, 4.789453699584773, 4.475792970019146, 4.166273337999092]

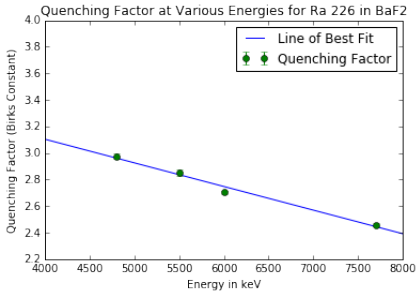

Figure 11: UV with filter Quenching Factors

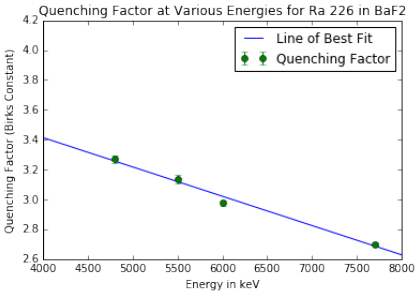

Figure 12: UV Quenching Factors

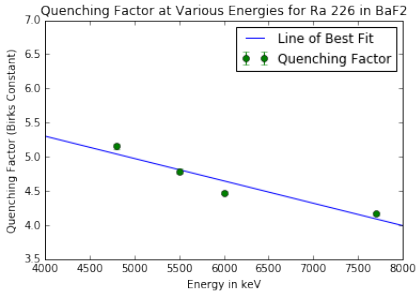

Figure 13: Solarblind Quenching Factors

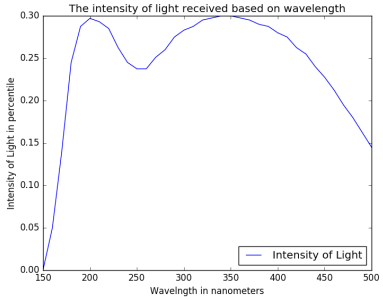

Figure 14: UV Quenching Factors

The emmission spectrum of Barium Flouride was plotted and fitted with four

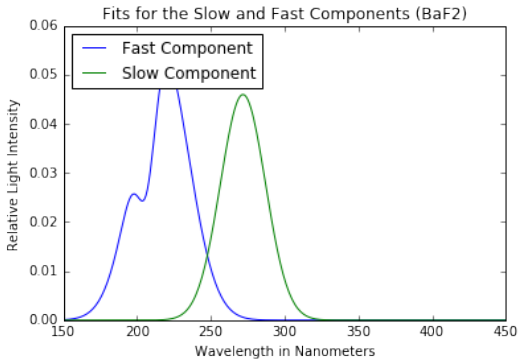

Figure 17: Solarblind Convolution

gaussians. Using this fit we convolved each QE spectrum [Figure 14] to find E_f and E_s [Figures 15 to 17].

Fast and Slow Proportions UV with filter = (0.10416262087647044, 0.8958373791235295) Fast and Slow Proportions UV = (0.11286243062670365, 0.8871375693732964) Fast and Slow Proportions Solarblind = (0.5585223540278348, 0.4414776459721652)

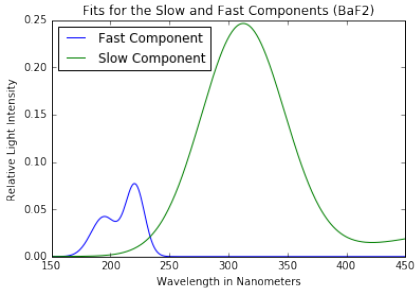

Figure 15: UV with filter Convolution

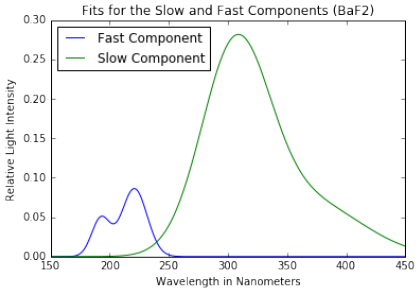

Figure 16: UV Convolution

We plotted our determined values in this form at each energy $\alpha_Q = E_f * \alpha_f + E_s * \alpha_s$ [Figures 18 to 21]. Solving for the best (α_s, α_f) at each energy level the quneching factor as a function of energy was found to be $\alpha_s = -0.1398072 * Energy + 4.13497323$ and $\alpha_f = -0.45007859 * Energy + 11.23363402$ with errors of $\sigma_s = [1.36287, 1.31089, 1.2333, 1.10977]$ and $\sigma_f = [0.0290772, 0.0310162, 0.0319127, 0.0313639]$ [Figure 22]. These functions can be used in future high energy physic experiments to isolate the fast component in BaF_2. Beyond experimental analysis on the quenching factor, the physical phenomenom that determine the constant will be explored.

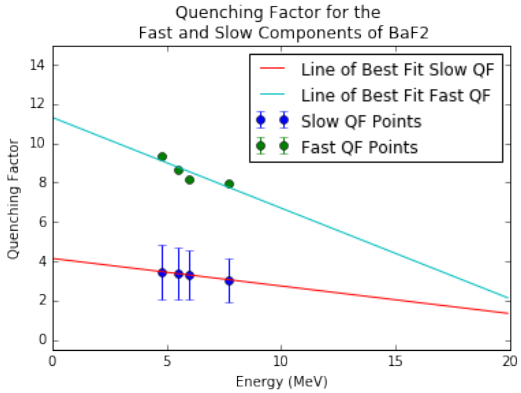

Figure 22: Final Quenching Factor Function

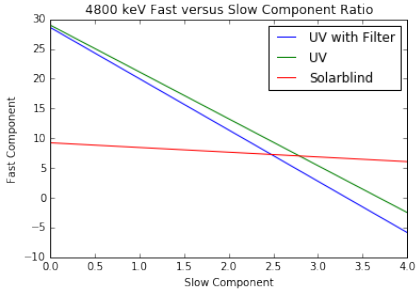

Figure 18: 4800 Slow versus Fast Componets

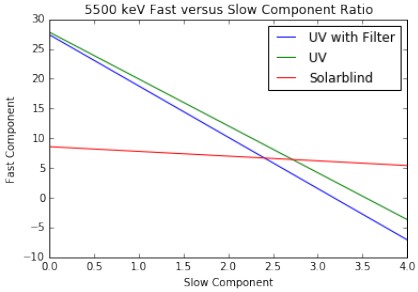

Figure 19: 5500 Slow versus Fast Componets

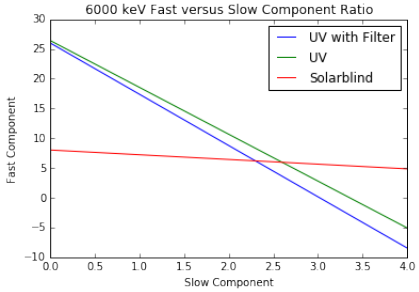

Figure 20: 6000 Slow versus Fast Componets

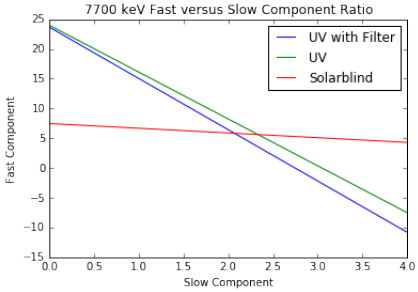

Figure 21: 7700 Slow versus Fast Componets

5 Acknowledgements

The measurement of the quenching factor for barium fluoride crystals was made possible by the California Institue of Technology and its Student Faculty Programs office for the Summer Undergraduate Research Fellowship. The involvement and support of Professor David Hitlin, Jake Kim, and Jason Trevor and the High Energy Physics group was crucial to the completion and implementation of this research.